Mismatched Disturbance Attenuation of a Spatially Developing Free Shear Flow

Christophe Collewet, Johan Carlier

Mismatched Disturbance Attenuation of a Spatially Developing Free Shear Flow

Christophe Collewet*† and Johan Carlier*†
*INRAE, UR OPAALE, Rennes Cedex F-35042, France
Email: firstname.name@inrae.fr
†Inria, Fluminance group, Rennes Cedex F-35044, France
Email: firstname.name@inria.fr

***Abstract*—This paper deals with the closed-loop control of a free shear flow subjected to mismatched disturbances. The goal is to maintain it in a desired state whatever the disturbances. Our approach consists of linearizing the Navier-Stokes equations about the desired state and next to perform a discretization step to obtain a linear state formulation. The components of the state vectors are the stream function evaluated at different points of the space assumed to be estimated via image techniques. The proposed control law writes as the sum of two terms. The first one allows to impose a behavior in regulation while the second one describes a behavior in attenuation. We show that this second term writes simply as a feedback gain that has to apply to the perturbation vector. However, since we consider that the disturbance is unknown, we propose a disturbance observer to derive the control law. Next, we prove the input-to-state stability of our control scheme. Simulations results on the DNS (direct numerical simulation) solver Incompact3d validate our approach.**

***Index Terms*—Closed-loop control, free shear flow, mismatched disturbances, observer based-control, visual servoing**

I. Introduction

Fluid flow control is widely used in lot of different application areas. For instance, in aviation laminarization is investigated to reduced the drag in order to reduce fuel consumption (see e.g. [1]). In the road transport, the same objective is expected (see e.g. [2]). Performance improvement of wind turbines is also expected, see [3] for a recent review. In contrast, in other application domains such as industrial chemistry, turbulence phenomena are encouraged to improve heat exchange [4] or to enhance chemical reactions or combustion performance [5].

Fluid flows are infinite dimensional systems described by partial differential equations (PDEs). The field of PDE control systems design has recently emerged as an important field of research in both applied mathematics and automatic control. However, this is a very daunting task due to the inherent difficulty of the Navier-Stokes equations and for now it could only be approached in some simplified particular cases (see [6] among others) or for more simple PDEs (see e.g. [7], [8]). Therefore, the common design approach assumes a first stage of linearization and spatial discretization, followed by a second stage of controller design based on classical control theory as in [9].

In this paper, we focus on the case of a spatially developing plane shear layer. This flow is induced by two parallel incident streams with different velocities separated by a thin plate where the actuator is located. This flow is known to be convectively unstable and to be a typical noise amplifier, leading to a very high sensitivity to upstream boundary conditions, see Fig. 1. Therefore, acting on the upstream conditions is an efficient way to enhance or reduce mixing due to turbulence. To do that, we have first linearized the Navier-Stokes equations about a desired state and then performed a spatial discretization to transform this set of partial differential equations to an ordinary set of linear differential equations. In addition, we assume that the state can be completely measured by image techniques (known as optical flow techniques) leading to a consistant state vector according to the physics of the flow (details are given in [10]). This approach is known as a visual servoing approach.

Since this flows is an amplifier, we propose in this paper a way to attenuate the consequences of an input disturbance. Contrary to our previous work where the matched case was considered [11], that is the disturbance evolves into the same space as the actuator one, the mismatched case is here studied. As in [11], we assume that the disturbance is unknown, but, in addition, we consider here the case where its spatial distribution is also unknown. To do that, a disturbance observer is introduced in the control law. The input-to-state (ISS) stability of the whole control scheme is proven under very weak conditions for the linearized system but simulation results will prove that this assumption is valid.

This paper is structured as follow. Section II is devoted to the modeling of the flow according to control issues. The problem of disturbance rejection / attenuation is detailed in Section III. The proposed disturbance observer is detailed in Section IV. The ISS stability is discussed in Section V. Section VI validates our approach through simulations results.

II. Modeling for flow control

The non dimensionalized Navier-Stokes equations and the continuity equation of an incompressible flow and Newtonian fluid are given by

$$\left\{\begin{array}{rcl}\partial_t \mathbf{u} + (\mathbf{u}.\nabla)\,\mathbf{u} & = & -\nabla p + \dfrac{1}{R_e}\Delta \mathbf{u} \\ \nabla \mathbf{u} & = & 0\end{array}\right. \quad (1)$$

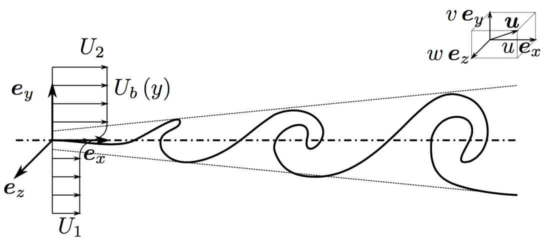

Fig. 1. A small disturbance is amplified in the streamwise direction.

where $\mathbf{u} = [u \quad v \quad w]^\top$ is the velocity vector at point $\mathbf{X} = [x \quad y \quad z]^\top$; p being the pressure at $\mathbf{X}$; R_e is a dimensionless number called the Reynolds number. The x-axis is associated to the streamwise direction, the y-axis to the normal direction and the z-axis to the spanwise direction of the flow (see Fig. 1).

We attach to the separated plate the following frame $(O, \mathbf{e}_x, \mathbf{e}_y, \mathbf{e}_z)$ where vector $\mathbf{e}_i$ is pointing along the direction of i-axis ($i \in \{x, y, z\}$). We assume that the stream below the separated plate writes as: $\mathbf{U}_1 = U_1\mathbf{e}_x$ with U_1 a constant value, while the stream above the separated plate writes as: $\mathbf{U}_2 = U_2\mathbf{e}_x$ with U_2 also a constant value (see Fig. 1).

To perform the nondimensionalization of the system (1), we used $U_0 = U_2 - U_1$, the volumetric mass density ρ_0 and the initial thickness of the shear layer δ_0. Therefore, the dynamic viscosity λ writes as the inverse of the Reynolds number $R_e = \rho_0 U_0 \delta_0/\lambda$.

Next, we proceed as proposed in our previous paper [11] and refer to this paper for more details. In [11], we considered the case where the flow was subject to small variations about a steady state leading to the velocity field vector $\mathbf{U}_b$ and the pressure P_b according to

$$\begin{cases} (\mathbf{U}_b.\nabla)\,\mathbf{U}_b &= -\nabla P_b + \dfrac{1}{R_e}\Delta \mathbf{U}_b \\ \nabla \mathbf{U_b} &= 0. \end{cases} \tag{2}$$

$\mathbf{U}_b$ can be obtained by an approximation of the Blasius solution of (2): $\mathbf{U}_b = [U_b \quad 0 \quad 0]^\top$ with $U_b = U_1 + \frac{1}{2}(\tanh(2y) + 1)$.

As in [11], we consider the case of a 2D flow such that the stream function $\psi(\mathbf{x}, t)$ in $\mathbf{x} = [x, y]^\top$ can be introduced to derive the well known vorticity-stream function formulation [12] of the linearized system (1) about $\mathbf{U}_b$:

$$\Delta\dot{\psi} = \mathcal{D}\psi, \tag{3}$$

where $\mathcal{D} = \left(-U_b\partial_x\Delta + d^2U_b/dy^2\partial_x + \frac{1}{R_e}\Delta^2\right)$ is a differential operator acting on ψ. The stream function ψ is defined from

$$\begin{cases} \delta u = +\partial_y \psi & \text{(4a)} \\ \delta v = -\partial_x \psi & \text{(4b)} \end{cases}$$

with δu the x component and δv the y component of the vector $\boldsymbol{\delta}\mathbf{u} = \mathbf{u} - \mathbf{U}_b$. Consequently, $\boldsymbol{\delta}\mathbf{u}$ describes the small variations of $\mathbf{u}$ about $\mathbf{U}_b$.

A. Boundaries Conditions

To effectively solve (3) one needs to specify the boundary conditions, that is the boundary of the study area defined by its dimensions L_x along x and L_y along y. We used Dirichlet boundary conditions at the inlet ($x = 0$), at the outlet ($x = L_x$) and at the top and bottom ($y = \pm\frac{L_y}{2}$):

- At the inlet, $\psi(\mathbf{x}, t)|_{x=0}$ is imposed by the stream function profil of the disturbance $\psi_d(\mathbf{x}, t)|_{x=0}$ and the stream function profil deduced from the control law $\psi_q(\mathbf{x}, t)|_{x=0}$. Thus, we have:

$$\psi\,(\mathbf{x}, t)\,|_{x=0} = \psi_d(\mathbf{x}, t)|_{x=0} + \psi_q(\mathbf{x}, t))|_{x=0}\;. \tag{5}$$

- At the outlet, the conditions are given trough the resolution of the following convection equation:

$$\left(\partial_t + \big(U_1 + \frac{1}{2}\big)\partial_x\right)\psi(\mathbf{x}, t)|_{x=L_x} = 0\;. \tag{6}$$

- At the top and bottom boundaries, assuming that no disturbance and no action occur, we can write:

$$\psi\,(\mathbf{x}, t)\,|_{y=\pm\frac{L_y}{2}} = 0. \tag{7}$$

B. Modeling for control issue

To explicitly reveal in (3) the parameters associated with the control law and with the disturbance terms, we transform the ordinary non homogenous differential equation (3) into a homogenous one by setting:

$$\psi(\mathbf{x}, t) = \psi_h(\mathbf{x}, t) + \psi_q(\mathbf{x}, t) + \psi_d(\mathbf{x}, t) \tag{8}$$

where ψ_h is the solution of the new ordinary homogenous differential equation. This equation is obtained by substituting (8) in (3):

$$\begin{aligned} \Delta\dot{\psi}_h(\mathbf{x}, t) \;&=\; \mathcal{D}\psi_h(\mathbf{x}, t) - \Big(\Delta\dot{\psi}_q(\mathbf{x}, t) - \mathcal{D}\psi_q(\mathbf{x}, t)\Big) - \\ &\quad \Big(\Delta\dot{\psi}_d(\mathbf{x}, t) - \mathcal{D}\psi_d(\mathbf{x}, t)\Big)\,. \end{aligned} \tag{9}$$

As proposed by several authors (e.g. [13]), we assume that the control and disturbance terms write as separable functions of time and space:

$$\begin{cases} \psi_q(\mathbf{x}, t) = f(\mathbf{x})q(t) \\ \psi_d(\mathbf{x}, t) = g(\mathbf{x})d(t) \end{cases} \tag{10}$$

where f and g are penetrating functions. They respectively model the way the actuator and the disturbance spatially impact the flow.

Considering (10), (9) becomes:

$$\begin{aligned} \Delta\dot{\psi}_h(\mathbf{x}, t) \;&=\; \mathcal{D}\psi_h(\mathbf{x}, t) - \Delta f(\mathbf{x})\dot{q}(t) + \mathcal{D}f(\mathbf{x})q(t) - \\ &\quad \Delta g(\mathbf{x})\dot{d}(t) + \mathcal{D}g(\mathbf{x})(\mathbf{x})d(t). \end{aligned} \tag{11}$$

To obtain a linear formulation of (11), a spatial discretization step is required. To do that, a finite difference scheme has been used. More precisely, the stream function ψ_h has been discretized on a cartesian mesh of size $n = n_x \times n_y$ according to high-order compact schemes leading to

$$\mathbf{L}\dot{\boldsymbol{\psi}}_h(t) = \mathbf{M}\boldsymbol{\psi}_h(t) + \mathbf{F}\dot{q}(t) + \mathbf{F}_D q(t) + \mathbf{G}\dot{d}(t) + \mathbf{G}_D d(t) \tag{12}$$

where $\boldsymbol{\psi}_h = \left[[\psi_{h\,1,1} \cdots \psi_{h\,n_x,1}] \cdots [\psi_{h\,1,n_y} \cdots \psi_{h\,n_x,n_y}]\right]^\top$ with $\psi_{h\,i,j} = \psi_h(x_i, y_j)$. $\mathbf{L}$ and $\mathbf{M}$ are full rank $(n \times n)$-dimensional matrices while $\boldsymbol{\psi}_h$, $\mathbf{F}$, $\mathbf{F}_D$, $\mathbf{G}$ and $\mathbf{F}_D$ are n-dimensional vectors.

Since $\mathbf{L}$ is full rank, (12) can be rewritten more simply as follows:

$$\dot{\boldsymbol{\psi}}_h(t) = \mathbf{A}\boldsymbol{\psi}_h(t) + \mathbf{B}_1\dot{q}(t) + \mathbf{B}_2 q(t) + \mathbf{B}_3\dot{d}(t) + \mathbf{B}_4 d(t) \quad (13)$$

with $\mathbf{A} = \mathbf{L}^{-1}\mathbf{M}$, $\mathbf{B}_1 = \mathbf{L}^{-1}\mathbf{F}$, $\mathbf{B}_2 = \mathbf{L}^{-1}\mathbf{F}_D$, $\mathbf{B}_3 = \mathbf{L}^{-1}\mathbf{G}$ et $\mathbf{B}_2 = \mathbf{L}^{-1}\mathbf{G}_D$.

However, this equation is not suitable to effectively control a flow. Indeed, $\boldsymbol{\psi}_h$ cannot be measured, only $\boldsymbol{\psi}$ (given by (8)) can be. Noting that the terms $\dot{q}(t)$ and $\dot{d}(t)$ in (13) come from the Laplacian operator applied to (10), the vector $\mathbf{z}$ defined by

$$\mathbf{z}(t) = \boldsymbol{\psi}_h(t) - \mathbf{B}_1 q(t) - \mathbf{B}_3 d(t) \quad (14)$$

is nothing but a spatial discretized approximation of $\boldsymbol{\psi}$ which is measurable for example by image-based techniques as mentioned in the introduction.

Finally, (13) becomes

$$\dot{\mathbf{z}}(t) = \mathbf{A}\mathbf{z}(t) + \mathbf{B}_q q(t) + \mathbf{B}_d d(t) \quad (15)$$

with $\mathbf{B}_q = \mathbf{A}\mathbf{B}_1 + \mathbf{B}_2$ et $\mathbf{B}_d = \mathbf{A}\mathbf{B}_3 + \mathbf{B}_4$.

In the next section we will focus on the way to attenuate the consequences of the disturbance on the flow.

III. Mismatched disturbance rejection

A. General case

In a more general case, the scalar $q(t)$ and $d(t)$ become vectors: respectively the m-dimensional vector $\mathbf{q}(t)$ and the r-dimensional vector $\mathbf{d}(t)$ leading to the $n \times m$ matrix $\mathbf{B}_q$ and to the $n \times r$ matrix $\mathbf{B}_d$ instead of vectors. Therefore, we have:

$$\dot{\mathbf{z}}(t) = \mathbf{A}\mathbf{z}(t) + \mathbf{B}_q\mathbf{q}(t) + \mathbf{B}_d\mathbf{d}(t). \quad (16)$$

We consider of course the case where the matrices $\mathbf{B}_q$ are $\mathbf{B}_d$ different, this case is known in the literature as the "mismatched case".

In order to specify different behaviors in regulation and rejection, the control law is split into two parts:

$$\mathbf{q}(t) = \mathbf{u}(t) + \mathbf{v}(t) \quad (17)$$

where $\mathbf{u}(t)$ will regulate to zero the state vector $\mathbf{z}(t)$ while $\mathbf{v}(t)$ will be devoted to counteract the disturbance $\mathbf{d}(t)$. Without loss of generality, we consider the case where $\mathbf{u}$ writes as a state feedback $\mathbf{u}(t) = -\mathbf{K}_z\mathbf{z}(t)$. Moreover, by plugging (17) in (16), we have

$$\dot{\mathbf{z}}(t) = (\mathbf{A} - \mathbf{B}_q\mathbf{K}_z)\mathbf{z}(t) + \mathbf{B}_q\mathbf{v}(t) + \mathbf{B}_d\mathbf{d}(t). \quad (18)$$

The matrix gain $\mathbf{K}_z$ is of course computed to ensure that $\mathbf{A} - \mathbf{B}_q\mathbf{K}_z$ is Hurwitz. Therefore, to reject the disturbance $\mathbf{d}(t)$, we have to find $\mathbf{v}(t)$ such that $\mathbf{B}_q\mathbf{v}(t) + \mathbf{B}_d\mathbf{d}(t) = \mathbf{0}$. This problem has been studied by Johnson [14]. Indeed, Johnson has shown that $\mathbf{B}_q\mathbf{v}(t) + \mathbf{B}_d\mathbf{d}(t) = \mathbf{0}$ if, and only if, $\mathbf{B}_d$ writes as:

$$\mathbf{B}_d = \mathbf{B}_q\boldsymbol{\Gamma} \quad (19)$$

where $\boldsymbol{\Gamma}$ is a $m \times p$ matrix. In that case, it is straightforward to show that the control law $\mathbf{v}(t) = -\boldsymbol{\Gamma}\mathbf{d}(t)$ ensures the convergence of the state to zero even if a disturbance $\mathbf{d}(t)$ occurs (in the case of course where $\mathbf{d}(t)$ is perfectly known).

Otherwise, the designer of the control law has no other choice than to attempt to minimize the effect of the disturbance while ensuring that the closed-loop system remains simply stable since the asymptotic stability of (18) can no longer be reached. We will return to this important problem at section V.

B. Case of the mixing layer

In that case, only one actuator is available, thus $m = 1$. We consider also the case where the magnitude of the disturbance $d(t)$ is scalar and constant, that is $d(t) = d$, $\forall t$ and above all unknown. In addition, we consider that $\mathbf{B}_d$ is also unknown since the penetrating function g involved in (10) is assumed to be unknown. Thus, (18) becomes

$$\dot{\mathbf{z}}(t) = \mathbf{A}_{cl}\mathbf{z}(t) + \mathbf{B}_q v(t) + \mathbf{W} \quad (20)$$

in which we have $\mathbf{A}_{cl} = \mathbf{A} - \mathbf{B}_q\mathbf{K}_z^\top$ and $\mathbf{W} = \mathbf{B}_d d$.

It is obvious that (19) is not verified for any given penetrating function g. Thus, we propose to minimise $J = \| \mathbf{B}_q v(t) + \mathbf{W} \|^2$ to limit the effect of the disturbance $\mathbf{W}$ on the flow. The control law is obtained by expressing the minimum of J with respect to $v(t)$:

$$\frac{\partial J}{\partial v(t)} = 2\mathbf{B}_q^\top\mathbf{B}_q v(t) + 2\mathbf{B}_q^\top\mathbf{W} \quad (21)$$

which gives:

$$v^* = -\mathbf{K}_w^\top\mathbf{W} \quad (22)$$

with

$$\mathbf{K}_w^\top = \frac{\mathbf{B}_q^\top}{\mathbf{B}_q^\top\mathbf{B}_q}. \quad (23)$$

It is of course a minimum since $\frac{\partial^2 J}{\partial^2 v(t)} = \mathbf{B}_q^\top\mathbf{B}_q$ is a positive scalar. In addition, let us point out that the gain $\mathbf{K}_w$ is a constant vector, thus it can be computed off-line.

Consequently, the whole control law (17) writes simply as a state feedback added by a feedback operating on the disturbance:

$$\mathbf{q}(t) = -\mathbf{K}_z^\top\mathbf{z}(t) - \mathbf{K}_w^\top\mathbf{W}. \quad (24)$$

Remark: In the matched case, we have $\mathbf{W} = \mathbf{B}_q d$ where, once having been plugged into (22), leads to $v^* = -d$ and to $J = 0$. We recover here that the control law perfectly counteracts the disturbance.

Since the control law (24) depends on the disturbance vector $\mathbf{W}$, it is essential to estimate it as best as possible. It is the issue of the next section.

IV. Disturbance observer

We extend here the observer proposed in [15]. Indeed, in [15], $\mathbf{B}_d$ involved in (15) is known. Thus, our observer is able to estimate as well the magnitude of the disturbance as its spatial distribution. Moreover, we present here a simpler derivation.

A way to express the problem is to try to ensure an asymptotic decrease of the observation error $\widetilde{\mathbf{W}}(t)$ defined as follow:

$$\widetilde{\mathbf{W}}(t) = \widehat{\mathbf{W}}(t) - \mathbf{W}. \tag{25}$$

This can be done by imposing an exponential decrease of the error:

$$\dot{\widetilde{\mathbf{W}}}(t) = -\lambda \widetilde{\mathbf{W}}(t), \quad \lambda > 0 \tag{26}$$

where λ is also used to tuned the convergence rate.

Thereafter, by plugging (25) in (26) and taking into account that $\mathbf{W}$ is constant, we have

$$\dot{\widehat{\mathbf{W}}}(t) = -\lambda \left(\widehat{\mathbf{W}}(t) - \mathbf{W} \right). \tag{27}$$

In the previous relation, $\mathbf{W}$ is not known, but it is involved in

$$\dot{\mathbf{z}}(t) = \mathbf{A}\mathbf{z}(t) + \mathbf{B}_q \mathbf{q}(t) + \mathbf{W} \tag{28}$$

which yealds

$$\dot{\widehat{\mathbf{W}}}(t) = -\lambda \left(\widehat{\mathbf{W}}(t) - \dot{\mathbf{z}}(t) + \mathbf{A}\mathbf{z}(t) + \mathbf{B}_q \mathbf{q}(t) \right). \tag{29}$$

However, in the above formulation the time derivative of the space is required. To remove this dependency, the following change of variable based on the one proposed in [15] is used:

$$\boldsymbol{\xi}(t) = \widehat{\mathbf{W}}(t) - \lambda \mathbf{z}(t) \tag{30}$$

leading to $\dot{\boldsymbol{\xi}}(t) = \dot{\widehat{\mathbf{W}}}(t) - \lambda \dot{\mathbf{z}}(t)$ which becomes by using the expression of $\dot{\widehat{\mathbf{W}}}(t)$ from (29):

$$\dot{\boldsymbol{\xi}}(t) = -\lambda \left(\widehat{\mathbf{W}}(t) + \mathbf{A}\mathbf{z}(t) + \mathbf{B}_q \mathbf{q}(t) \right) \tag{31}$$

which simplifies by expressing $\widehat{\mathbf{W}}(t)$ from (30) as follows:

$$\dot{\boldsymbol{\xi}}(t) = -\lambda \left(\boldsymbol{\xi}(t) + \lambda \mathbf{z}(t) + \mathbf{A}\mathbf{z}(t) + \mathbf{B}_q \mathbf{q}(t) \right). \tag{32}$$

This last expression gives the final formulation of the disturbance observer:

$$\left| \begin{array}{rcl} \widehat{\mathbf{W}}(t) & = & \boldsymbol{\xi}(t) + \lambda \mathbf{z}(t) \\ \dot{\boldsymbol{\xi}}(t) & = & -\lambda \big(\boldsymbol{\xi}(t) + \lambda \left(\mathbb{I}_n + \mathbf{A} \right) \mathbf{z}(t) + \mathbf{B}_q \mathbf{q}(t) \big). \end{array} \right. \tag{33}$$

It is clear that it is an asymptotic observer since it has been designed to satisfy (26).

Finally, the control law (24) becomes

$$\mathbf{q}(t) = -\mathbf{K}_z^\top \mathbf{z}(t) - \mathbf{K}_w^\top \widehat{\mathbf{W}}(t). \tag{34}$$

The next section is devoted to the stability analysis of (20) controlled by (34).

V. Stability Analysis

When no disturbance occurs, the equilibrium point $\mathbf{z} = \mathbf{0}$ is asymptotically stable for the linearized closed-loop system. In contrast, as it has been shown in III-A, when it is disturbed the state cannot converge anymore to $\mathbf{z} = \mathbf{0}$.

We will show in this section that, if the disturbance remains bounded, the state will be also bounded. This propriety is known in the literature as the ISS stability and has been first introduced by Sontag for nonlinear systems [16].

Let us recall the equations governing the linearized closed-loop system:

$$\begin{cases} \dot{\mathbf{z}}(t) &= \mathbf{A}\mathbf{z}(t) + \mathbf{B}_q \mathbf{q}(t) + \mathbf{W} & \text{(35a)} \\ \mathbf{q}(t) &= -\mathbf{K}_z^\top \mathbf{z}(t) - \mathbf{K}_w^\top \widehat{\mathbf{W}}(t) & \text{(35b)} \\ \dot{\widetilde{\mathbf{W}}}(t) &= -\lambda \widetilde{\mathbf{W}}(t) & \text{(35c)} \\ \widetilde{\mathbf{W}}(t) &= \widehat{\mathbf{W}}(t) - \mathbf{W} & \text{(35d)} \end{cases}$$

which gives by plugging (35b) in (35a):

$$\dot{\mathbf{z}}(t) \quad = \mathbf{A}_{cl} \mathbf{z}(t) - \mathbf{B}_q \mathbf{K}_w^\top \widehat{\mathbf{W}}(t) + \mathbf{W} \tag{36}$$

and by expressing $\widehat{\mathbf{W}}(t)$ from (35d):

$$\begin{cases} \dot{\mathbf{z}}(t) = \mathbf{A}_{cl} \mathbf{z}(t) - \mathbf{B}_q \mathbf{K}_w^\top \widetilde{\mathbf{W}}(t) + \left(\mathbb{I}_n - \mathbf{B}_q \mathbf{K}_w^\top \right) \mathbf{W} & \text{(37a)} \\ \dot{\widetilde{\mathbf{W}}}(t) = -\lambda \widetilde{\mathbf{W}}(t) & \text{(37b)} \end{cases}$$

that we can treat as the following augmented system:

$$\dot{\boldsymbol{\zeta}}(t) = \bar{\mathbf{A}} \boldsymbol{\zeta}(t) + \bar{\mathbf{B}} \mathbf{W} \tag{38}$$

where $\boldsymbol{\zeta}(t) = \left[\mathbf{z}(t), \widetilde{\mathbf{W}}(t) \right]^\top$ and

$$\bar{\mathbf{A}} = \begin{bmatrix} \mathbf{A}_{cl} & -\mathbf{B}_q \mathbf{K}_w^\top \\ \mathbf{0} & -\lambda \mathbb{I}_n \end{bmatrix}, \bar{\mathbf{B}} = \begin{bmatrix} \mathbb{I}_n - \mathbf{B}_q \mathbf{K}_w^\top \\ \mathbf{0} \end{bmatrix}. \tag{39}$$

For an initial condition $\boldsymbol{\zeta}(t) = \boldsymbol{\zeta}_0$, an explicit solution of (38) can be obtained:

$$\boldsymbol{\zeta}(t) = e^{\bar{\mathbf{A}}(t - t_0)} \boldsymbol{\zeta}_0 + \int_{t_0}^{t} e^{\bar{\mathbf{A}}(t - \tau)} \bar{\mathbf{B}} \mathbf{W} d\tau. \tag{40}$$

Since: (i) the matrix $\mathbf{A}_{cl}$ is Hurwitz by construction, (ii) the matrix $-\lambda \mathbb{I}_n$ is Hurwitz since $\lambda > 0$, therefore the matrix $\bar{\mathbf{A}}$ is also Hurwitz. Thereafter, $\| e^{\bar{\mathbf{A}}t} \|$ is bounded for any $t > 0$ and there exist two positive constants k and μ such that

$$\| e^{\bar{\mathbf{A}}(t - t_0)} \| \le k e^{-\mu(t - t_0)}. \tag{41}$$

Consequently, we have

$$\| \boldsymbol{\zeta}(t) \| \le k e^{-\mu(t-t_0)} \| \boldsymbol{\zeta}_0 \| + k \int_{t_0}^{t} e^{-\mu(t-\tau)} \| \bar{\mathbf{B}} \| \| \mathbf{W} \| d\tau \tag{42}$$

and finally

$$\| \boldsymbol{\zeta}(t) \| \le k e^{-\mu(t-t_0)} \| \boldsymbol{\zeta}_0 \| + \frac{k \| \bar{\mathbf{B}} \|}{\mu} \| \mathbf{W} \|. \tag{43}$$

Therefore, for any bounded constant disturbance $\mathbf{W}$, the state of the system controlled by (35b) is also bounded.

In addition, we have

$$\lim_{t \to +\infty} \| \boldsymbol{\zeta}(t) \| \le \frac{k \| \bar{\mathbf{B}} \|}{\mu} \| \mathbf{W} \|. \tag{44}$$

Remark: It is easy to verify that $\mathbf{K}_w$ given by (23) minimizes also $\| \bar{\mathbf{B}} \|$ in (44).

VI. Simulation Results

The whole control scheme has been implemented in the Navier-Stokes equations solver Incompact3d [17]. It solves (1) according to the boundaries conditions detailed in section II-A and taking (10) into account.

The control law has been computed from (35b). The gain $\mathbf{K}_z$ has been computed by resolution of the Ricatti equation to derive a classical LQR control law (more details are given in [11]). The penetrating functions f and g (see section II-B) are defined such that $f(\mathbf{x}) = \exp\left((-x/4)^2\right)h_f(y)$ and $g(\mathbf{x}) = \exp\left((-x/4)^2\right)h_g(y)$ where the fonctions h_f and h_g are plotted in Fig. 2 (more details concerning these choices are also given in [11]). These figure clearly shows that we are in the mismatched case ($\mathbf{B}_q \neq \mathbf{B}_d$): $h_g(y)$ cannot be deduced from $h_f(y)$ by a constant coefficient. The estimation of the disturbance (its magnitude and its spatial distribution $g(\mathbf{x})$) is obtained thanks to the observer described by the set of equations (33) (λ has been set to 5). The value of the Reynolds number has been set to 300, the value of n_x was 64 while the value of n_y was 32.

To evaluate both the relevance of using a linearized system and the behavior of the observer, we have introduced the following error signal: $E_{\mathbf{W}} = \widetilde{\mathbf{z}}_{k+1}^\top \widetilde{\mathbf{z}}_{k+1}$ where $\widetilde{\mathbf{z}}_{k+1} = \mathbf{z}_{k+1} - \widehat{\mathbf{z}}_{k+1}$. The vector $\widehat{\mathbf{z}}_{k+1}$ is obtained by integration of the following dynamic system:

$$\dot{\widehat{\mathbf{z}}}(t) = \mathbf{A}\mathbf{z}(t) + \mathbf{B}_q q(t) + \widehat{\mathbf{W}}(t) \tag{45}$$

between $t = kT$ and $t = (k+1)T$ where $q(t)$ and $\widehat{\mathbf{W}}(t)$ are assumed to be constant during the integration time. T has been set to 0.1 in dimensionless time. The initial condition concerning $\mathbf{z}(t)$ is given by the Navier-Stokes solver at $t = kT$: $\mathbf{z}_k = \mathbf{z}(kT)$ as well as $\mathbf{z}_{k+1} = \mathbf{z}((k+1)T$. Indeed, if $\widehat{\mathbf{W}}(t)$ converges to the true value $\mathbf{W}$ and if our approach of linearization is valid, then $E_{\mathbf{W}}$ will tend to zero.

Fig. 3 depicts the behavior of the mixing layer when the disturbance is assumed to be occurred at $t = 0$ and with $\mathbf{z}(0) = \mathbf{0}$. As can be seen in Fig. 3a, $\|\mathbf{z}(t)\|^2$ is very affected by the disturbance when no control law is applied (in red), as well as only a state feedback control law is applied (in green). In contrast, the proposed control scheme is very efficient since $\|\mathbf{z}(t)\|^2$ has been drastically decreased (in blue). However, in the three cases, the same behavior is observed. The state vector is growing during the transient step until the steady state is reached. The duration of the transient state is around 30 in dimensionless time.

Let us detail more precisely the way the control scheme is used in practice. Fig. 3b depicts the behavior of $\mathbf{K}_w^\top \widehat{\mathbf{W}}(t)$ at the very beginning of the simulation, its convergence to a stable value does not occur immediately, consequently we propose to take $\widehat{\mathbf{W}}(t)$ into account in the control law only when a stable value is reached. In practice, it happens for $t = t^*$ (approximately 1.1 in this simulation). Then, for $t < t^*$ only the state feedback is applied. Next, for $t \geq t^*$, the compensation term $\mathbf{K}_w^\top \widehat{\mathbf{W}}(t)$ is used. In addition, to avoid a discontinuity in the control law we use:

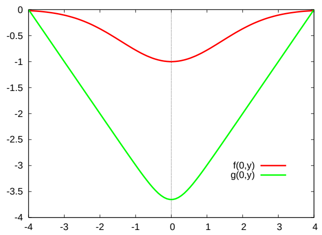

Fig. 2. Penetrating functions $f(\mathbf{x})$ and $g(\mathbf{x})$ at $x = 0$.

$$\mathbf{q}(t) = -\mathbf{K}_z^\top \mathbf{z}(t) - H(t - t^*)\left(1 - e^{-\frac{t-t^*}{\tau}}\right)\mathbf{K}_w^\top \widehat{\mathbf{W}}(t) \tag{46}$$

where $H(.)$ is the Heaviside function. The parameter τ has been set to a small value ($\tau = 1$) to ensure that the compensation term $v(t)$ is quickly reached. Fig. 3c depicts the behavior of the control law (46).

Fig. 3d details the behavior of $\log_{10}(E_{\mathbf{W}})$ with (in green) or without compensation term (in red). First, these signals decrease rapidly until they reach a plateau corresponding to the duration of the transient step. That means that some non linearities occur since $\mathbf{K}_w^\top \widehat{\mathbf{W}}(t)$ has already reached its convergence value (see Fig. 3e). Once the transient step is finished, $E_{\mathbf{W}}$ vanishes and consequently also $\widetilde{\mathbf{W}}(t)$, but that also means that the state vector obtained from the linearized model is very closed to the ground true given by the Navier-Stokes equations solver. This result proves that even if $\mathbf{z}$ is relatively high (see Fig. 3a, and it is especially the case when only the LQR control is applied), the linearized model is still valid in the steady state.

Fig. 4 confirms that our approach is valid even for state vectors far from the desired state about which the linearization has been performed. Indeed, in this 2nd simulation the magnitude of the disturbance is twice the one in the previous simulation. As can be seen in Fig. 4a, using a compensation term is still very efficient. Moreover, here again, $E_{\mathbf{W}}$ have the same behavior than in the previous simulation and of course the same conclusion can be drawn. In addition, for the first simulation we have $z_\infty^2 = \lim_{t\to+\infty} \|\mathbf{z}(t)\|^2 = 31.0708$ while for the 2nd one we have $z_\infty^2 = 128.0328$ (when using the compensation term in the control law). Thus, we have almost a factor 4 between the two steady states. Consequently, even if the flow has been very affected by the disturbance, it behaves like the linearized system. Indeed, it is easy to show from (37a) that in that case z_∞ is directly proportional to $\mathbf{W}$.

Remarks: The control law (46) is of course robust with respect to t^*. However, the sooner a valid compensation term is applied, the lower the value of the maximum of $\|\mathbf{z}(t)\|^2$ is. The control law (46) is also robust with respect to τ. This parameter is involved in the instantaneous energy consumption of the actuator. A compromise has then to be done between energy consumption and efficiency to limit the influence of the disturbance.

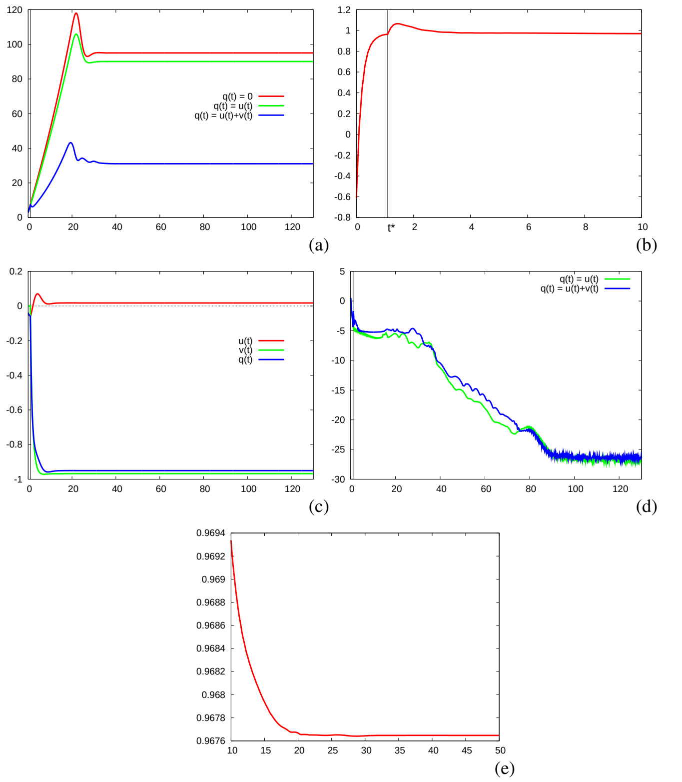

Fig. 3. Closed-loop control of the mixing layer (x axes in dimensionless time). (a) Norm of the state vector vs. time ; (b) Compensation term $\mathbf{K}_w^\top \widehat{\mathbf{W}}(t)$ vs. time ; (c) Control signal vs. time ; (d) Behavior of $\log_{10}(E_{\mathbf{W}})$ vs. time; (e) Zoom on $\mathbf{K}_w^\top \widehat{\mathbf{W}}(t)$ vs. time.

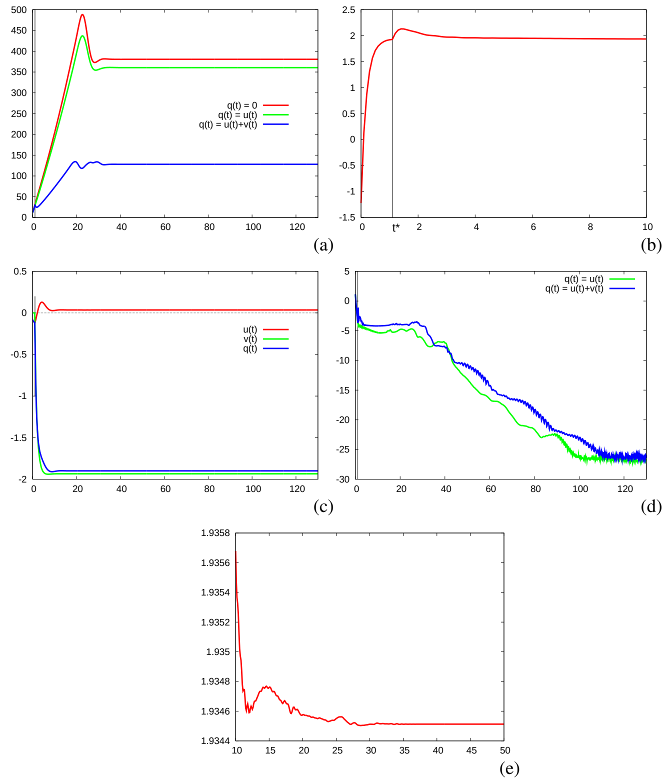

Fig. 4. 2^{nd} Simulation (the figures have the same meaning as in Fig. 3).

VII. Conclusion and Future Works

We have proposed a control scheme of a mixing layer flow subject to mismatched disturbances. Our approach allows to attenuate the influence of a completely unknown disturbance, that is as well its magnitude as its spatial distribution. To do that, we have designed an observer that leads to an estimation of the whole disturbance (magnitude and spatial distribution). Next, this estimation is used in the control law. The proof of the ISS stability has been given considering the linearized system under very simple conditions. Unfortunately, the extension of our result to the Navier-Stokes equation seems to be out of reach. Nevertheless, simulation results on a Navier-Stokes equations solver have proven that our approach based on linearization is valid.

Future work will concern the case where disturbances are slowly times varying. We plan also to validate our approach on our wind tunnel.

References

[1] J. C. Lin, E. A. Whalen, J. Eppink, E. Siochi, M. Alexander, and M. Andino, "Innovative flow control concepts for drag reduction," in *54th AIAA Aerospace Sciences Meeting*. San Diego, California, USA: American Institute for Aeronautics and Astronautics, 4-8 January 2016.

[2] R. Li, B. Noack, L. Cordier, J. Borée, and F. Harambat, "Machine learning control for drag reduction of a car model in experiment," in *20th IFAC World Congress*, Toulouse, France, July 2017, pp. 14 154–14 157.

[3] S. Aubrun, A. Leroy, and P. Devinant, "A review of wind turbine-oriented active flow control strategies," *Experiments in Fluids*, vol. 58, no. 10, September 2017.

[4] A. Messaadi, E. Dorignac, M. Fénot, and J.-J. Vullierme, "Aerothermal characteristics of a mixing layer on a multiperforated plate," in *Proceedings of ASME Fluids Engineering Division Summer Meeting 2006, FEDSM2006*, vol. 1, July 2006.

[5] C. Bekdemir, B. Somers, and P. De Goey, "DNS with detailed and tabulated chemistry of engine relevant igniting systems," *Combustion and Flame*, vol. 161, no. 1, pp. 210–221, 2014.

[6] R. Vazquez and M. Krstić, "A closed-form feedback controller for stabilization of the linearized 2-d navier–stokes poiseuille system," *IEEE Transactions on Automatic Control*, vol. 52, no. 12, pp. 2298–2312, 2007.

[7] J. Deutscher and C. Harkort, "A parametric approach to finite-dimensional control of linear distributed-parameter systems," *International Journal of Control*, vol. 83, no. 8, pp. 1674–1685, August 2010.

[8] M. Krstić, "Adaptive control of anti-stable wave pde systems: Theory and applications in oil drilling," in *11th IFAC International Workshop on Adaptation and Learning in Control and Signal Processing*, University of Caen Basse-Normandie, Caen, France, July 2013, pp. 432–439.

[9] L. Baramov, O. Tutty, and E. Rogers, "H_∞ control of nonperiodic two-dimensional channel flow," *IEEE Transactions on Control Systems Technology*, vol. 12, no. 1, pp. 111–122, January 2004.

[10] R. Tatsambon Fomena and C. Collewet, "Fluid flow control: a vision-based approach," *Int. Journal of Flow Control*, vol. 3, no. 2, pp. 133–169, 2011.

[11] D. Anda-Ondo, J. Carlier, and C. Collewet, "Closed-loop control of a spatially developing free shear flow around a steady state," in *20^{th} IFAC World Congress*, Toulouse, France, July 2017.

[12] P. J. Schmid and D. S. Henningson, *Stability and transition in shear flows*, ser. Applied Mathematical Sciences, 142. New York: Springer-Verlag, 2001.

[13] S. Joshi, J. L. Speyer, and J. Kim, "A system theory approach to the feedback stabilization of infinitesimal and finite amplitude disturbances in plane Poiseuille flow," *J. Fluid Mech.*, vol. 332, pp. 157–184, 1997.

[14] C. D. Johnson, "Accommodation of external disturbances in linear reg-

ulator and servomechanism problem," *IEEE Transactions on Automatic Control*, vol. 16, no. 5, pp. 635–644, December 1971.
[15] W.-H. Chen, D. J. Ballance, P. J. Gawthrop, J. J. Gribble, and J. O'Reilly, "Nonlinear PID predictive controller," *IEE Proc-Control Theory Appl.*, vol. 146, no. 6, pp. 603–611, 1999.
[16] E. D. Sontag, "Smooth stabilization implies coprime factorization," *IEEE Trans. on Automatic Control*, vol. 34, no. 4, pp. 435–443, 1989.
[17] S. Laizet and E. Lamballais, "High-order compact schemes for incompressible flows: A simple and efficient method with quasi-spectral accuracy," *J. Comput. Phys.*, vol. 228, no. 16, pp. 5989–6015, 2009.